

Resonance of Spike Discharge Modulation in Neurons of the Guinea Pig Medial Vestibular Nucleus

L. RIS,² M. HACHEMAOUI,¹ N. VIBERT,¹ E. GODAUX,² P. P. VIDAL,¹ AND L. E. MOORE¹

¹Laboratoire de Neurobiologie des Réseaux Sensorimoteurs, Centre National de la Recherche Scientifique, Université Paris 5, ESA 7060, 75270 Paris Cedex 06, France; and ²Laboratory of Neurosciences, University of Mons-Hainaut, B-7000 Mons, Belgium

Received 31 January 2001; accepted in final form 5 April 2001

Ris, L., M. Hachemaoui, N. Vibert, E. Godaux, P. P. Vidal, and L. E. Moore. Resonance of spike discharge modulation in neurons of the guinea pig medial vestibular nucleus. *J Neurophysiol* 86: 703–716, 2001. The modulation of action potential discharge rates is an important aspect of neuronal information processing. In these experiments, we have attempted to determine how effectively spike discharge modulation reflects changes in the membrane potential in central vestibular neurons. We have measured how their spike discharge rate was modulated by various current inputs to obtain neuronal transfer functions. Differences in the modulation of spiking rates were observed between neurons with a single, prominent after hyperpolarization (AHP, type A neurons) and cells with more complex AHPs (type B neurons). The spike discharge modulation amplitudes increased with the frequency of the current stimulus, which was quantitatively described by a neuronal model that showed a resonance peak >10 Hz. Modeling of the resonance peak required two putative potassium conductances whose properties had to be markedly dependent on the level of the membrane potential. At low frequencies (≤ 0.4 Hz), the gain or magnitude functions of type A and B discharge rates were similar relative to the current input. However, resting input resistances obtained from the ratio of the membrane potential and current were lower in type B compared with type A cells, presumably due to a higher level of active potassium conductances at rest. The lower input resistance of type B neurons was compensated by a twofold greater sensitivity of their firing rate to changes in membrane potential, which suggests that synaptic inputs on their dendritic processes would be more efficacious. This increased sensitivity is also reflected in a greater ability of type B neurons to synchronize with low-amplitude sinusoidal current inputs, and in addition, their responses to steep slope ramp stimulation are enhanced over the more linear behavior of type A neurons. This behavior suggests that the type B MVNn are moderately tuned active filters that promote high-frequency responses and that type A neurons are like low-pass filters that are well suited for the resting tonic activity of the vestibular system. However, the more sensitive and phasic type B neurons contribute to both low- and high-frequency control as well as signal detection and would amplify the contribution of both irregular and regular primary afferents at high frequencies.

INTRODUCTION

Although many experimental and modeling studies have been done to characterize the membrane properties of central neurons, there is very little information on the biophysical

properties of intact neurons in a functioning network. The biophysical properties of neurons in their normal network environment are difficult to assess when action potentials are spontaneously firing. This situation especially applies to the vestibular system where the normal input from the vestibular hair cells causes a modulation of a spontaneous carrier discharge present in most vestibular neurons at “rest.” This modulation is responsible for the vestibulospinal and vestibuloocular reflex, VOR (Babalian et al. 1997; Curthoys 1982; Serafin et al. 1999; Vibert et al. 1997).

Since sensory vestibular input acts as a modulating stimulus, it is reasonable to simulate it by DC input to medial vestibular nucleus neurons (MVNn) to more precisely characterize the responses of central neurons. Our rationale is to determine how MVNn use the modulation of spontaneously occurring action potentials compared with simply responding as some type of signal detector or threshold device. Clearly the most relevant signals for network properties are action potentials and synaptic events, both of which are dependent on the entire neuronal structure. Since continuously firing neurons are likely to have different properties than those at rest, it is important to measure them during activity. This is a problem because most quantitative studies involve experimental conditions in which action potentials are either pharmacologically abolished or controlled in a voltage clamp. Thus the experiments described in this paper involve the development of quantitative techniques to use spike discharge rate as a measure of membrane properties to describe neuronal behavior in situ.

Measurements from guinea pig slices of MVNn have led to a classification of neurons based on membrane properties as expressed by their action potential profiles (Gallagher et al. 1985; Johnston et al. 1994; Serafin et al. 1991a). MVNn constitute a continuum of cells (du Lac and Lisberger 1995b; Johnston et al. 1994) in between two canonical classes that can be distinguished by the following characteristics: type A, having single large afterpotentials, and type B, which show more complex afterpotentials including fast and slow components. In slices, the firing frequencies are reasonably constant for both A and B neurons (see Table 1, $C_v\%$) in contrast to their presumed behavior in intact preparations where B units are thought to be much more irregular (Babalian et al. 1997). Typically, these

Address for reprint requests: L. E. Moore, Laboratoire de Neurobiologie des Réseaux Sensorimoteurs, CNRS ESA 7060, 45 rue des Saint Pères, 75270 Paris Cedex 06, France (E-mail: moore@ccr.jussieu.fr).

The costs of publication of this article were defrayed in part by the payment of page charges. The article must therefore be hereby marked “advertisement” in accordance with 18 U.S.C. Section 1734 solely to indicate this fact.

TABLE 1. Spike discharge modulation parameters for type A and B neurons

	Type A	Type B	P	Types A and B
R_h , M Ω	67 \pm 42 (21)	63 \pm 28 (20)	1.0	65 \pm 36 (41)
IF_r , spikes/s	28 \pm 21 (28)	29 \pm 17 (27)	0.8	28 \pm 19 (53)
C_v , %	10 \pm 12 (20)	11 \pm 12 (25)	0.8	10 \pm 11 (45)
IF_r/IF_m	4.1 \pm 3.1 (14)	3.6 \pm 0.2 (18)	0.9	3.8 \pm 2.2 (32)
$\delta IF(4 \text{ Hz})/\delta IF(0.4 \text{ Hz})$	1.20 \pm 0.1 (10)	1.4 \pm 0.2 (17)	0.1	1.3 \pm 0.2 (27)
Overshoot, spikes/s	1.9 \pm 1.8 (9)	5.6 \pm 5.6 (10)	0.08	3.8 \pm 4.5 (19)
$R_{\text{active}}(0.4 \text{ Hz})$, M Ω	50 \pm 28 (15)	23 \pm 16 (19)	0.006	35 \pm 25 (34)
$\delta IF/\delta I(0.4 \text{ Hz})$, spikes \cdot s $^{-1}$ \cdot nA $^{-1}$	128 \pm 58 (13)	140 \pm 48 (19)	0.4	131 \pm 54 (32)
$\delta IF/\delta V(0.4 \text{ Hz})$, spikes \cdot s $^{-1}$ \cdot mV $^{-1}$	3.3 \pm 2.4 (13)	6.8 \pm 3.8 (19)	0.007	5.4 \pm 3.7 (32)

Mean values with their SDs, number of neurons (in parentheses) and unpaired *t*-test *P* values are given for the type A and B neurons: R_h , the input resistance measured with a 500-ms pulse during a maintained hyperpolarization of the neurons in M Ω ; IF_r , resting action potential firing rate in spikes/s; C_v , the coefficient of per cent variation of the resting firing rate; IF_r/IF_m , ratio of the resting firing rate vs. the maximum frequency of modulation of this firing rate; $\delta IF(4 \text{ Hz})/\delta IF(0.4 \text{ Hz})$, ratio between the amplitudes of the modulations of the action potential firing rate for the same amplitude current input at 4 and 0.4 Hz; Overshoot is the difference between the peak instantaneous frequency at the end of a 600-ms ramp current and the final value of IF at the same current applied for 2 s. $R_{\text{active}}(0.4 \text{ Hz})$, the input resistance in M Ω measured during the sinusoidal modulation at 0.4 Hz of action potential discharge; $\delta IF/\delta I(0.4 \text{ Hz})$, ratio of the modulation of the spike discharge in spikes/s vs. the injected current in nA at 0.4 Hz; $\delta IF/\delta V(0.4 \text{ Hz})$, ratio of the modulation of the spike discharge in spikes/s vs. the membrane potential change induced by sinusoidal stimulation at 0.4 Hz.

neurons are spontaneously active and appear to function as frequency modulators in response to vestibular input (Serafin et al. 1991a). In addition, empirical models of type A and B neurons (Av-Ron and Vidal 1999; Quadroni and Knöpfel 1994) suggest that these two classes of cells should show a difference in their experimentally measured frequency modulation (FM) (Ris et al. 1998) corresponding to a specific relation between intrinsic membrane properties and network function. For instance, a particular type B model, but not A, simulated a resonant behavior above 10 Hz (Av-Ron and Vidal 1999). The membrane properties required for type B neuronal behavior, and the results obtained on the isolated whole brain preparation are consistent with the hypothesis that the irregular, phasic firing behavior observed in vivo (Shimazu and Precht 1965) is likely to be associated with type B neurons and regular tonic activity with type A cells (Babalian et al. 1997).

Previous intracellular measurements on vestibular neurons of chick slices (du Lac and Lisberger 1995a) showed good sinusoidal modulation of spiking rates in response to sinusoidal current injections and essentially linear behavior. In addition, the spike discharge modulation of vestibular neurons showed increasing amplitudes with increasing stimulating frequency. Similarly, increasing peak discharge rates have been observed in visual cortical neurons (Carandini et al. 1996) for neurons that only fire during the depolarizing part of current sine waves. Thus these latter neurons rectify and do not show good modulation of a spontaneous discharge rate, which is either very low or nonexistent. Nevertheless, whether or not there is a good modulation of a spontaneous firing rate, virtually all resting neurons show an increase in their peak, instantaneous discharge rates as the current stimulation frequency increases. These results strongly suggest that the underlying membrane potential response must also be increasing, since higher peak discharge rates generally occur with membrane depolarization. These findings are completely different from the passive membrane potential responses that are obtained from the same cells, both vestibular and cortical, during a maintained hyperpolarization that abolishes spontaneous activity. Therefore it seems likely that the increase in peak spike discharge with an increase in sinusoidal stimulating frequency is due to active voltage-dependent properties of the membrane channels.

It is indeed important to emphasize the difference between passive and active *linear* responses. Passive responses always show decreasing amplitudes as the frequency is increased; however, active linear responses may show an increase in amplitude to a peak resonant value and then decrease with frequency. We have found that most neurons show an increase in the amplitude of spike discharge modulation as the stimulating frequency is increased, which is likely to be the consequence of an enhanced underlying sinusoidal membrane potential response. At the usual spontaneous discharge rates of 30 Hz and above, it is difficult to determine the potential response since it is mixed with the components of the afterpotentials following each spike. At lower spontaneous discharge rates the potential response can be determined using spectral analysis (Carandini et al. 1996) because the dominant frequency of the signal is at the stimulating frequency; however, this is not the case at higher discharge rates. Therefore we have restricted our analysis to instantaneous frequencies since we are only considering responses that show FM for both the depolarizing and hyperpolarizing phases of the stimulating current inputs.

In this paper, we have characterized vestibular neurons by their responses to step, ramp, and small sinusoidal inputs over a range of different steady-state conditions that are similar to those encountered in normal network behavior. This approach elicits both linear and nonlinear responses that can be used to evaluate models of intact neurons. In particular, we can quantitatively describe the linear modulation of spike discharge rates by small signals using the linear form of voltage-dependent neuronal models if we assume that the spike discharge is directly proportional to the membrane potential. Larger current inputs cannot be described by linear analysis and would require a complete nonlinear description using essentially all the voltage-dependent conductances present in the neuron. We will show that the sinusoidal linear responses of type B neurons have a greater increase in their modulation amplitude with frequency than the type A neurons. At higher frequencies the type B neurons behave like signal detectors that fire only during depolarization.

METHODS

The experiments reported here were done with sharp microelectrodes on thick ($500\ \mu$) brain stem slices (Lewis et al. 1987, 1989) from adult guinea pigs. The experimental procedures were identical to those described by Serafin et al. (1991a) and were in accordance with the European Communities Council directive of November 24, 1986, and the procedures issued by the French Ministère de l'Agriculture. Only neurons from the medial vestibular nucleus were measured, taking the border of the IVth ventricle as a reference point (see Serafin et al. 1991a). All measurements were done with an Axoclamp 2A system in either the bridge or switching discontinuous current clamp (DCC) mode (Moore et al. 1999). The electrode resistance was 80–120 M Ω . Both series resistance (bridge balance) and capacitive compensation were used. The bridge balance was verified by demonstrating no change in the potential recording when switching between the continuous and discontinuous modes. Each neuron was characterized as type A or B according to their action potential profiles (see Fig. 1A) as previously described (Serafin et al. 1991a). Figure 1 illustrates the traditional method of stimulating with a constant current and recording a membrane potential response. The constant current stimuli (Fig. 1D) consisted of sine waves from 0.2 to 20 Hz, which gave an underlying sinusoidal potential response that was less than 10 mV peak to peak. This frequency range was used in order to remain well

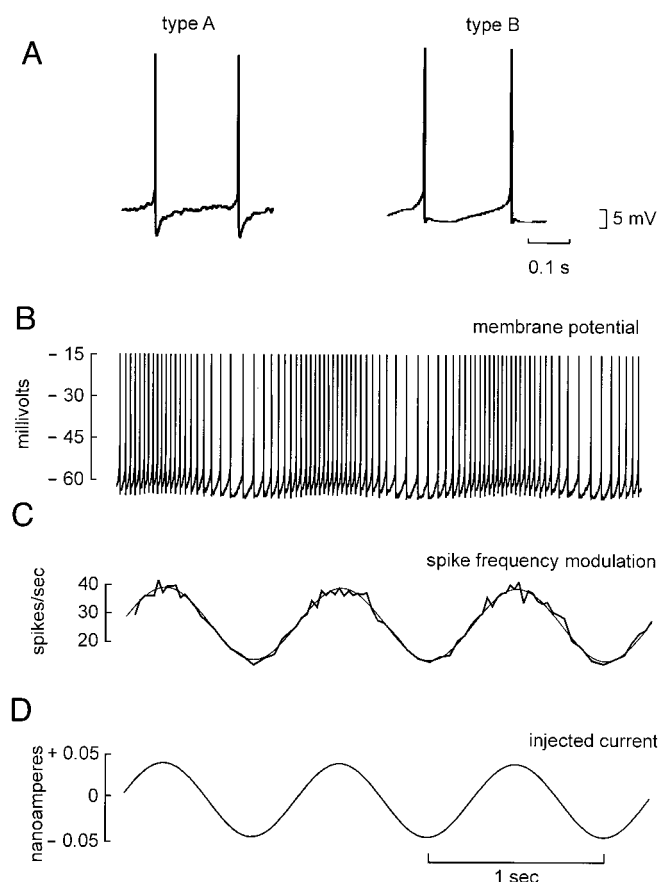


FIG. 1. Measurement of spike discharge modulation for type A and B neurons. The recorded action potentials were used to classify type A and B neurons as illustrated in A by differences in negative afterpotentials. A sinusoidal current (D) was injected into the neurons to modulate the rate of impulse discharge (B). Instantaneous firing rates modulations were calculated and fitted with a sine wave (C) to obtain the magnitude and phase shifts at different stimulating frequencies, which were then fitted to a neuronal model. The spike discharge modulation amplitude (spikes/s) was expressed as an impedance magnitude (M Ω) by estimating the sinusoidal potential (B) excursion (~ 4 mV), which provided a measure of the input resistance ($50\ \text{M}\Omega = 4\ \text{mV}/0.08\ \text{nA}$) that was equivalent to the modulation amplitude of 25 spikes/s (see C).

below the spontaneous or carrier frequency, which imposed the limit in our measurement of the modulated responses. In addition, depolarizing or hyperpolarizing d.c. currents were superimposed on the sine waves to measure responses at different steady state membrane potentials. Finally, increasing ramp currents were applied at different slopes up to a final steady state value.

The typical response of these neurons at the resting potential is illustrated in Fig. 1 by a type B neuron that was stimulated with a constant current sine wave at 1 Hz. Figure 1C shows a fitted sine wave to the instantaneous firing rate (IF , spikes/s) that was calculated as the reciprocal of the interval between two successive action potentials. The IF was determined for all stimulus protocols with a Mathematica (Wolfram 1999) script that estimated the time intervals between action potentials based on the time of their peak value above a threshold value of -10 – 0 mV. The time at the end of each interval between action potentials was used to indicate the time for each IF value. The amplitude of the fitted sine wave and its phase relative to the current stimulus provide the experimentally determined frequency domain functions discussed in the following text.

Since the maximum stimulus frequency that will modulate the spiking rate is dependent on the level of the spontaneous discharge, which in turn can be modified by the level of membrane depolarization, it is necessary to experimentally determine the maximum frequency (IF_m) at which modulation is still observed. It should be emphasized that all the analyses of spike discharge responses to sinusoidal stimulation that are discussed in this paper were done only for those cases where instantaneous firing rate (IF) points were obtained for both the depolarizing and hyperpolarizing parts of each cycle of stimulation, i.e., the neuron never stopped firing, even during the hyperpolarizing phases of the current modulation. Thus IF_m is the maximum frequency that fits these criteria. The average spontaneous firing rates (IF_s) for type A and B neurons were not different in the slice preparation nor their coefficients of variation (C_v) expressed as percentage (Table 1). A good indication of the modulation capabilities of each neuron is the ratio between its spontaneous discharge (IF_s) and its maximum modulation frequency (IF_m). A ratio of ~ 3 – 4 was found for both type A and B neurons (Table 1). Thus this ratio is a reflection of the sampling rate showing that each instantaneous firing rate cycle is determined by three to four points (of spontaneous frequency), which seems reasonable since the sampling intervals cannot be equal. If the sampling intervals could have been equal, the theoretical Nyquist sampling limit would require a minimum of two sample points per cycle at the maximum frequency of the analysis (Marmarelis and Marmarelis 1978).

The data analysis consisted of an estimation of the spontaneous or carrier frequency and its modulation from 0.2 Hz to a maximum modulation frequency that varied from cell to cell, having a range from 3 to 15 Hz. The ratio, $\delta IF(4\ \text{Hz})/\delta IF(0.4\ \text{Hz})$ (Table 1), of the amplitudes of the spike discharge modulations at high (4 Hz) and low (0.4 Hz) frequencies were determined for each neuron. Selected parameters from the analysis are given in Table 1, which includes P values from unpaired t -tests (SYSTAT, SPSS, Chicago, IL) to evaluate the differences between type A and B neurons.

The range of mean membrane potentials and the maximum frequency for which vestibular neurons show modulation is quite variable. Neurons with spontaneous firing rates above 30 Hz showed reasonable FM up to ~ 10 Hz. Because frequency versus current (F/I) responses are relatively linear for limited displacements, it is reasonable to assume that spiking rates are proportional to small changes of the membrane potential. This simple assumption provides a method to measure the impedance of a neuron in its natural state, for each frequency of sinusoidal stimulation, by monitoring the changes in instantaneous firing rates. In addition, our analysis has been restricted to the linear range by limiting the current input to give a peak to peak membrane potential response < 10 mV. The extent of this linear IF range was verified by measuring its limits during current stimulation ramps having different slopes (see Fig. 8).

The calibration of the fitted *IF* responses versus the associated membrane potential changes requires an estimate of the peak-to-peak change in membrane potential associated with the change in *IF*. Since the instantaneous firing rate is assumed to reflect the membrane potential, this relationship between the changes in *IF* (δIF) and membrane potential (δV) was assumed constant. The calibration factor was estimated at 0.2–0.4 Hz by measuring the amplitude of the peak to peak excursion of both parameters during one stimulus cycle beginning at the minimum of the negative afterpotential (Fig. 1*B*). The stimulus strength was limited to assure that the form of the action potential did not change during the cycle. Only low stimulating frequencies were suitable for estimating underlying membrane potential changes because of the difficulty in determining the form of the sinusoidal response as the stimulating frequency approached the spiking rate. The ratio at low frequencies between the membrane potential variation (δV) in the presence of action potentials and the injected current (δI) was defined as the active input resistance, R_{active} (0.4 Hz in Table 1). The example of Fig. 1 indicates that the measured spike modulation amplitude (δIF) was 25 spikes/s (Fig. 1*C*), which corresponded to a membrane potential sinusoidal deflection of ~ 4 mV (Fig. 1*B*). With a peak-to-peak current of 0.08 nA (Fig. 1*D*), these values (25/4) would give a calibration factor of $6.25 \text{ spikes} \cdot \text{s}^{-1} \cdot \text{mV}^{-1}$ ($\delta IF/\delta V$) that converts a modulation of 25 spikes/s to an input resistance of $4 \text{ mV}/0.08 \text{ nA} = 50 \text{ M}\Omega$. As the peak-to-peak current underlying the sinusoidal stimulation at each frequency is constant, any difference in the amplitude of the action potential modulation at various frequencies will reflect a change in the natural impedance of the neuron. If the spike discharge modulation is assumed to be proportional to the membrane potential modulation, one can directly infer the impedance of the cell at each given frequency using the constant calibration factor, $\delta IF/\delta V$ (0.4 Hz). In addition to R_{active} , an input resistance at hyperpolarized levels, R_{h} , was obtained by superimposing a long duration (500 ms) current pulse on a steady-state hyperpolarization that had abolished action potentials (see Table 1). The associated membrane potential change was measured at the end of the pulse.

Thus the amplitude of the spike discharge modulation (δIF) induced at any frequency is divided by the calibration factor, $\delta IF/\delta V$ (0.4 Hz) (see Table 1), and then by the constant current, δI , to obtain the impedance, $Z(\delta V/\delta I)$, as a function of frequency. The measurement of Z involves both magnitude (gain) and phase functions, which are necessary for a complete description of the data that can then be used to indicate the presence or absence of active conductances. The calibration of the spike discharge data are required to allow a direct comparison with linearized neuronal models. This type of analysis provides estimates of both the active and passive parameters of the neuronal model (see APPENDIX) and validates the applicability of linear analysis for this data.

Linearity of the spiking rate modulation was tested by superimposing responses to different levels of sinusoidal current stimulation at the same frequency (du Lac and Lisberger 1995a; Marmarelis and Marmarelis 1978). In general, current levels that evoked peak membrane potential changes <5 – 10 mV were in a linear range. The NonLinearFit package of Mathematica (Wolfram Research, Champaign, IL) was used for fitting the *IF* data to single frequency sine waves.

RESULTS

Modulation properties of type A and B neurons

Neurons of the medial vestibular nucleus show spontaneously firing behavior in a slice preparation despite the obvious reduction of afferent input. These neurons can be distinguished from each other by the shape of their hyperpolarizing afterpotentials. Figure 1*A* illustrates examples of the two extreme

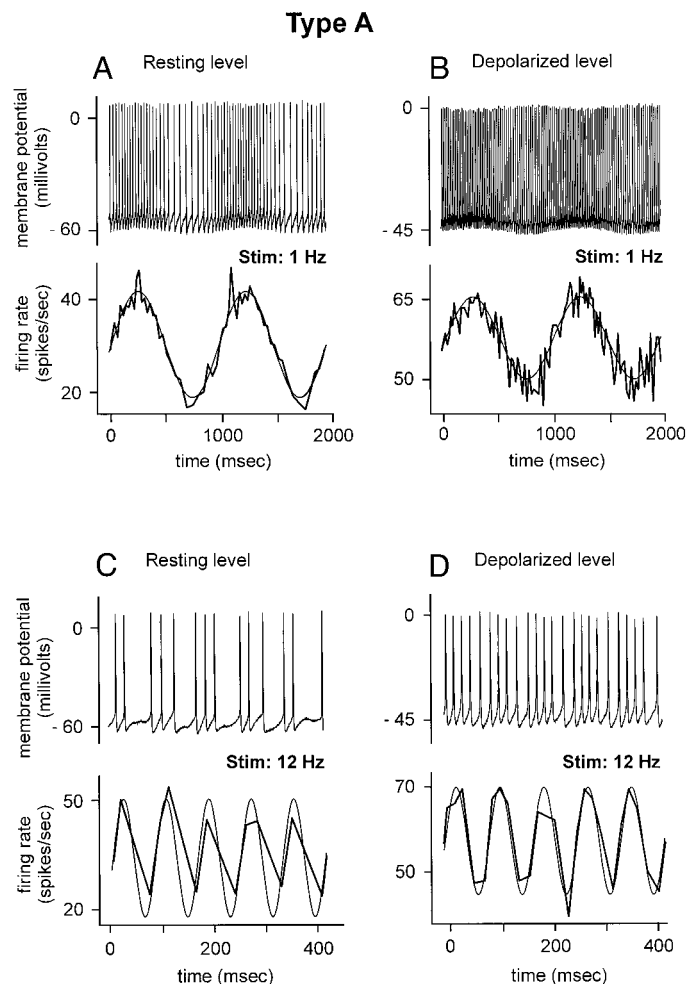


FIG. 2. Spike discharge modulation of a resting and depolarized type A neuron. Modulated action potential responses to sinusoidal current stimuli (sine amplitude of 0.09 nA) are shown for the indicated frequency ranges and analyzed by superimposing a fitted sine wave (smooth lines) on the instantaneous firing rate (spikes/s) derived from the spike records. The discharge modulation at rest (A) was effective up to 6 Hz in this type A cell; however, a maintained depolarization of 0.3 nA (B) increased the steady-state discharge from 30 (A and C) to 57 Hz (B and D) and increased the range of adequate modulation ≤ 12 Hz (D).

forms of afterpotentials (type A and B), both of which are present and regularly firing in the slice preparation. To simulate the effect of afferent input, sinusoidal current was injected into these cells to observe possible response differences between type A and B neurons. Figure 1*B* illustrates a type B neuron response to a 1-Hz current input. Figure 1*C* shows a fit of the sinusoidal instantaneous frequency (*IF*) demonstrating excellent modulation for both the depolarizing and hyperpolarizing portions of the response.

Figure 2*A* shows a corresponding type A neuron that modulates its spontaneous (carrier) frequency of ~ 30 Hz from 20 to 40 Hz for a displacement of the membrane potential of just a few millivolts. This modulation response is limited by the carrier frequency as is indicated by the imperfect modulation shown in Fig. 2*C* for a 12-Hz stimulus. Figure 2*B* illustrates that the dynamic range of this modulation can be significantly increased by a maintained depolarization, which nearly doubles the average steady state frequency to ~ 57 Hz. The practical advantage of this increased frequency is seen by the

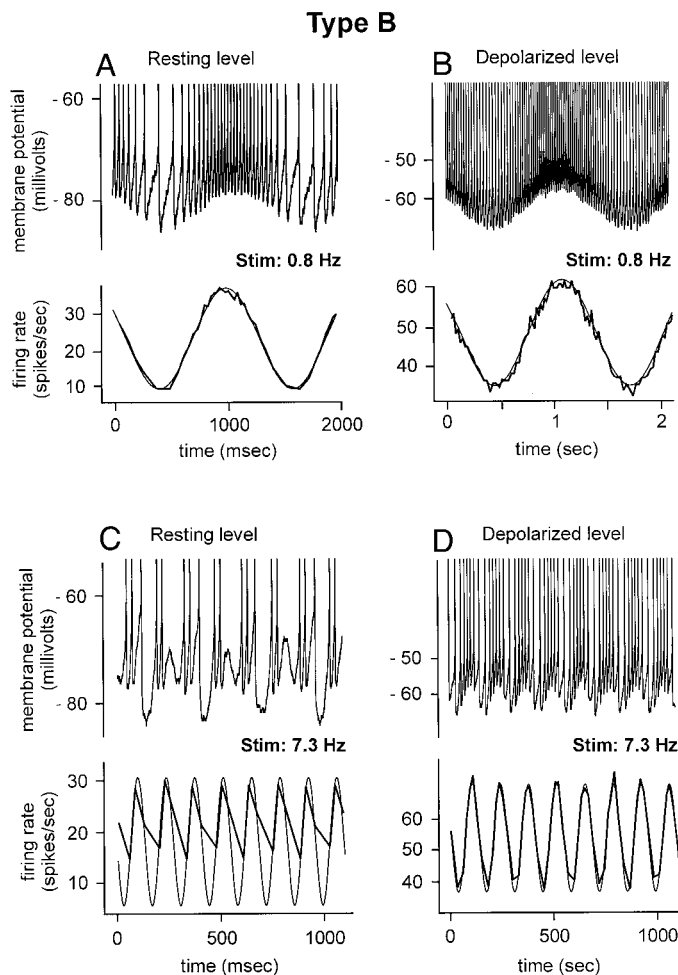


FIG. 3. Limits of spike discharge modulation of a resting and depolarized type B neuron. *A*: action potential responses to a 0.8-Hz sinusoidal current stimulus that invoked a modulation of the action potential firing rate. Instantaneous firing rate (spikes/s) analysis of *A*, top, and superimposed fitted sine wave (smooth lines). *B*: spike discharge modulation as in *A* but during a maintained depolarizing current of 0.5 nA. *C*: spike discharge modulation to a 7.3-Hz current stimulus. Instantaneous firing rate (spikes/s) analysis of *C* and superimposed fitted sine wave (smooth lines). *D*: the depolarized type B neuron shows significantly better modulation at 7.3 Hz. The stimulating current amplitude was 0.13 nA.

relatively good modulation response at a 12-Hz current input in Fig. 2*D*.

Figure 3, *A* and *B*, illustrates a type B neuron that shows good modulation at low frequencies; however, at 7.3 Hz, the modulation is insufficient even though the spontaneous carrier discharge was about threefold greater (Fig. 3*C*). The modulation is clearly restored if the spontaneous frequency is increased by a depolarization (Fig. 3*D*). Although the modulation at rest was inadequate, the instantaneous firing rates could be fitted with a sine wave that was synchronized with the stimulus current at 7.3 Hz (Fig. 3*C*). This illustrates an example where the amplitude of the fitted sine wave (7.3 Hz) is completely determined by the *IF* at the peak of the depolarization, which thus limits its accuracy. In these instances, the action potentials tend to occur on rising phase of the stimulating sine wave and thus show a phase lead. In another type B cell, synchronization on alternate cycles of a 10-Hz stimulus was observed (Fig. 4*C*). In this neuron, modulation was also restored by a depolariza-

tion that increased the carrier frequency (Fig. 4*D*). Thus although type B neurons show good modulation at low frequencies, they tend to fire in synchrony with the depolarizing phase of the stimulus when the stimulating frequency increases.

In contrast, at stimulation frequencies approaching the spontaneous firing rate, type A neurons showed a maintained but unsynchronized, relatively constant discharge. The neuron illustrated in Fig. 5 shows that the spontaneous discharge rate can be below high stimulating frequencies at its resting potential (Fig. 5*A*) or above it during a depolarization (Fig. 5*B*). Figure 5, *C* and *D*, shows the usual type B neuronal response of marked action potential synchronization to small sinusoidal currents both at resting and depolarized levels. Figure 5*B* shows that at a resting discharge level of ~25 Hz, the action potential responses were one for one with the 25-Hz stimulus, and at depolarized levels, the responses to each sine wave were doublet action potentials (Fig. 5*D*). In type A neurons, the lack of synchronization occurs above one-half of the spontaneous frequency; however, type B neurons remain synchronized at all stimulating frequencies. Thus the transition between modu-

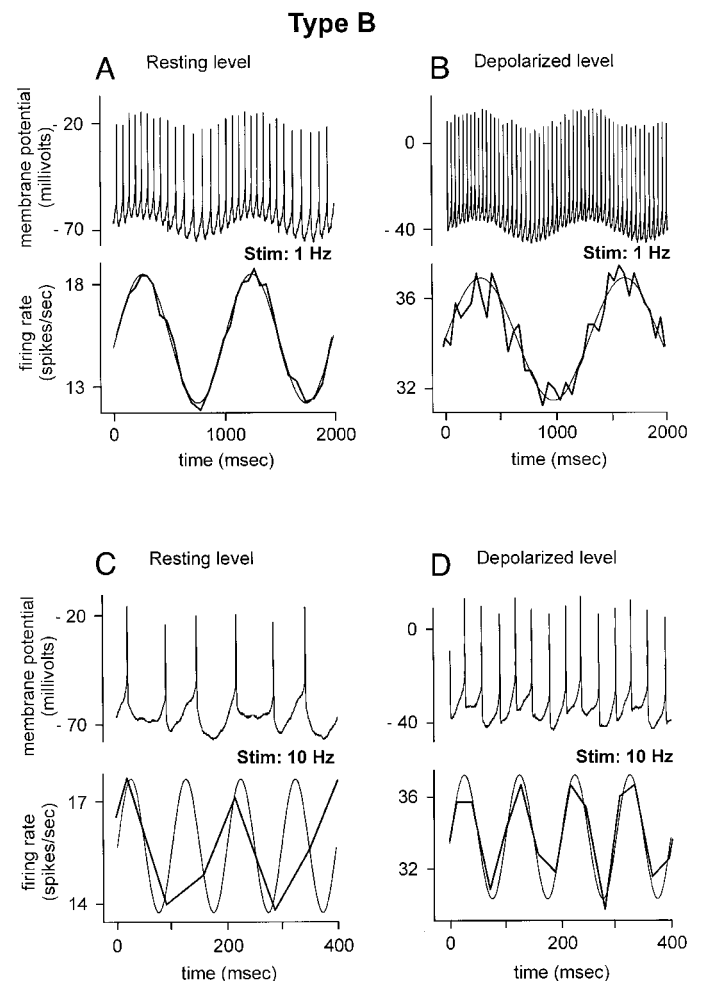


FIG. 4. Spike discharge modulation of a resting and depolarized type B neuron. *A*: spike discharge modulation to a 1-Hz stimulus with an amplitude of 0.13 nA. *B*: modulation during a maintained depolarization with 0.5 nA of steady state current. *C*: lack of modulation for a 10-Hz stimulus at the resting level. *D*: a 0.5-nA steady current depolarized the neuron and led to an increased discharge rate from 16 to 34 Hz. The higher steady-state action potential firing rate allowed significantly better modulation in the 5- to 10-Hz range compared with the resting neuron.

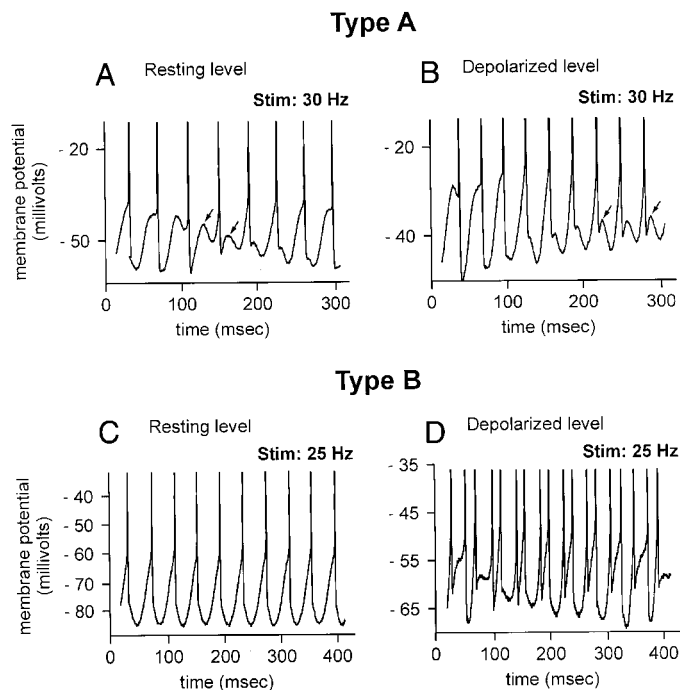


FIG. 5. Synchronization of type A and B neurons to stimulation frequencies. **A**: the type A response at 30 Hz indicates that this neuron was unable to synchronize with the 30-Hz stimulus frequency, as indicated by the \downarrow . The measured instantaneous firing rate was 28 Hz, just below the 30-Hz stimulation frequency. **B**: although an improvement in the discharge modulation at intermediate frequencies was observed for this and other type A neurons, synchronization did not occur at higher frequencies. The illustrated depolarized type A neuron had an instantaneous firing rate above the 30-Hz stimulus, which was clearly not in synchrony with the sine wave stimulus. **C** and **D**: the type B neuron shows very poor discharge modulation past 7 Hz (see Fig. 3); however, good synchronization of the response was seen at 25 Hz for both the resting (**C**) and depolarized conditions (**D**). In the latter instance, action potential doublets were observed.

lated and unmodulated responses are different for the two neuronal types.

Spike FM at low frequencies (<10 Hz) is clearly present in both type A and B neurons; however, type A neurons appear to have a more stable intrinsic firing pattern, which is controlled by the steady-state value of the membrane potential. Although type B neurons are reasonably regular in the slice preparation, they tend to have a lower amplitude after hyperpolarization potential with a greater sensitivity to external stimuli, which can lead to more irregular behavior (Av-Ron and Vidal 1999; Babalian et al. 1997). This increased sensitivity provides a means to synchronize responses with small stimuli and detect input signals at relatively high frequencies.

To compare type A and B neurons, the amplitude of the spike FM (δIF) was plotted as a function of frequency and current. Figure 6A illustrates that the amplitude of the spike discharge modulation of this type A neuron has a nearly constant response for frequencies from 0.2 to 14 Hz at current amplitude levels ≤ 0.5 nA. Above this current level, the type A response is nonlinear as indicated by an enhancement of the modulated response with an increase in frequency. By contrast, the type B neuron, illustrated in Fig. 6B, showed a significant enhancement of its amplitude responses with frequency at all current levels (≤ 0.3 nA). At these current levels the responses could be superimposed and were therefore linear.

To further illustrate the contrast between type A and B

neurons, the IF data were plotted relative to current rather than frequency in Fig. 6, **C** and **D**. The plots were done for different frequencies showing that the type A δIF s are nearly superimposed for low current levels; however, at current levels >0.3 nA, there is a nonlinear increase in δIF as the stimulating frequency is increased (Fig. 6C). Alternatively, the type B neuron of Fig. 6D shows an increase in δIF with stimulating frequencies >1 Hz at all levels of current amplitude. Both type A and B neurons show modulation and linear responses at low current levels (<0.3 nA). At higher current levels, type A neurons may continue to show modulated responses; however, they are clearly nonlinear. In many B neurons, it was not possible to obtain good modulation responses at high current levels >0.3 nA, as illustrated in Fig. 6D by the lack of points past 0.2 nA at 4 and 8 Hz. Under these conditions, the IF response is nonlinear because of rectification. In these instances, increasing the spontaneous frequency by depolarizing the neuron extended the linear range.

Thus in neuronal systems, linear versus nonlinear responses cannot be separated simply as a dependence of gain on frequency. However, an increase of gain with frequency is dependent on the activation of voltage-dependent conductances that can be linear or nonlinear depending on the size of the stimulus. In general, linearity can be evaluated by the usual criteria of superposition or scaling of responses relative to stimulus amplitude. Figure 6 shows that type A and B neurons are clearly different in their linear responses and that the nonlinear responses evoked in type A neurons at current levels >0.5 nA resemble the linear response of type B neurons at current levels <0.3 nA.

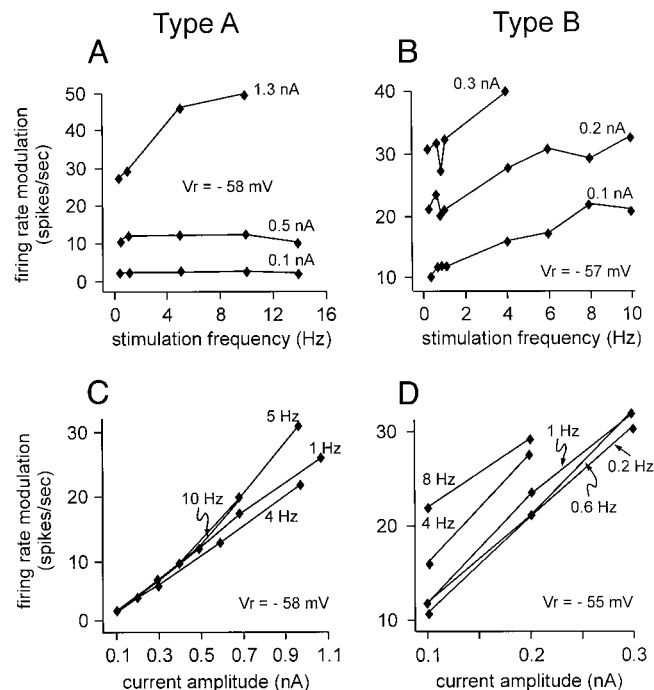


FIG. 6. Tests of linearity of type A and B neurons. **A**: the amplitude of a type A response in spikes/s of the modulated spiking rate is plotted as a function of the stimulating frequency for 3 current levels (0.1, 0.5, and 1.3 nA). **B**: type B spike discharge modulation amplitude responses to 3 sinusoidal current levels (0.1, 0.2, and 0.3 nA) are shown as a function of frequency. **C**: the amplitude of the type A response is plotted as a function of the current amplitude for 4 frequencies (0.4, 1, 5, and 10 Hz). **D**: similar type B responses are shown as a function of sinusoidal current amplitude.

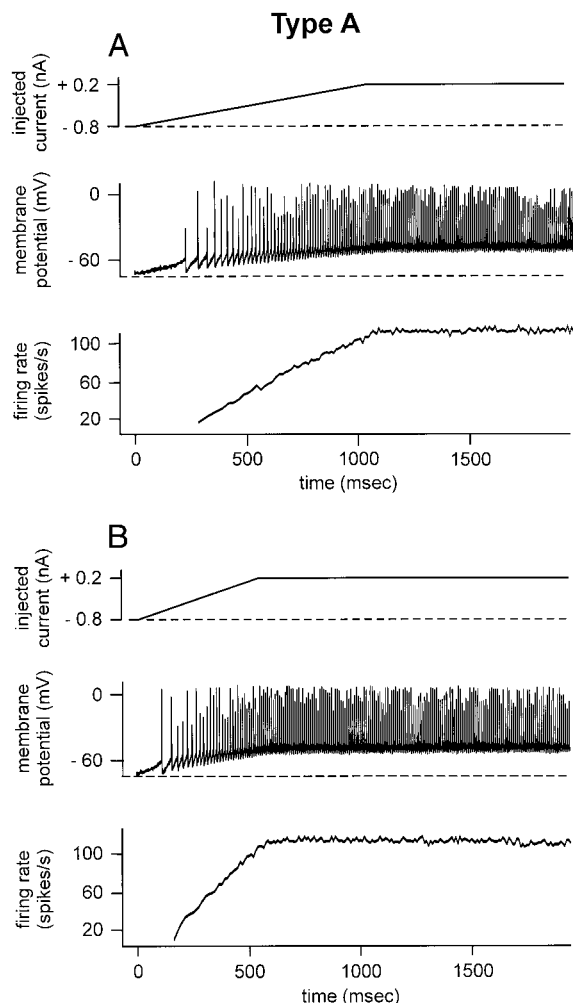


FIG. 7. Type A neuronal responses to ramp stimuli. *A*: a ramp current was given from a hyperpolarized level of -0.8 nA for 1 s to reach $+0.2$ nA. Action potential and instantaneous firing rates are given in the 2nd and 3rd traces, respectively, which show that the instantaneous firing rate follows the current without any overshooting response. *B*: a ramp current with a steeper slope ending at 0.5 s showed a similar response. In both cases, a slight decrease can be observed in the firing rate slopes during the positive depolarizing current, which is indicative of an activation of a potassium conductance. The final current level in each case was 0.2 nA, which induced a firing rate in excess of 100 spikes/s.

Ramp stimulation

The contrast in spike discharge responses (IF) to high-frequency sinusoidal stimulation between type A and B neurons can be dramatically illustrated by responses to ramp current (I_m) stimuli. Figure 7, *A* and *B*, illustrates that type A neurons in a hyperpolarizing range have a nearly linear IF response with time to a ramp current stimulus (-0.8 – 0 nA) for both high and low slopes. The IF response during the depolarizing part of the ramp starting at the resting membrane potential (0 – 0.2 nA) has a slightly lower slope compared with the hyperpolarized part of the ramp (-0.8 – 0 nA) but was nearly linear up to the maximal current with no overshooting response. The slightly lower slope of the spiking rate increase most likely represents the activation of a potassium conductance as the neuron is depolarized. Even though the instantaneous firing rate increased from 20 to 100 Hz, the current levels produced <20 mV membrane potential displacements

from the resting potential and appear to approximate linearity. The lack of an overshoot for ramps with different slopes suggests that the spike discharge response is not enhanced or diminished by rapid changes in the current and is thus consistent with a sinusoidal response whose amplitude is relatively constant with frequency. Table 1 indicates that type A neurons show an average overshoot of <2 spikes/s for a ramp duration of 600 ms.

The type B neuron of Fig. 8, *A* and *B*, shows a greater decrease in the slope (IF/I_m) for depolarizing versus hyperpolarizing currents and an overshoot in the instantaneous frequency compared with the final steady-state value that is achieved during the maintained maximum current. This overshoot is significantly enhanced at steep slopes (Fig. 8*B*), which reflects the augmentation in amplitude of spike discharge modulation observed with an increase (resonance) in sinusoidal stimulation frequencies. Thus during a steep ramp stimulation,

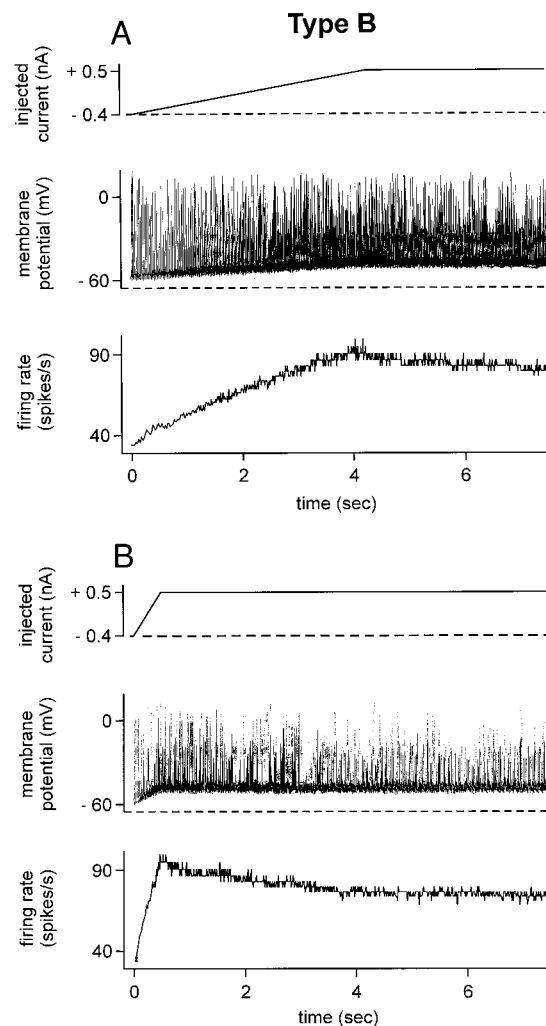


FIG. 8. Type B neuronal responses to ramp stimuli. *A*: a ramp current was given from a hyperpolarized level of -0.4 nA for 4.24 s to reach $+0.5$ nA. Action potential and instantaneous firing rates are given in the 2nd and 3rd traces respectively, which show that the instantaneous firing rate follows the current with a small overshooting response. *B*: a ramp current with a steeper slope ending at 0.5 s showed a pronounced overshooting response in the firing rate. In both cases, a decrease can be observed in the firing rate slopes during the positive depolarizing current, which is indicative of an activation of a potassium conductance. The final current level in each case was 0.5 nA, which induced a firing rate near 100 spikes/s.

the instantaneous firing rate is significantly enhanced over its steady-state value at any given potential. At the moment the dynamic stimulus stops and becomes constant, the firing rate (IF) is higher because of the high-frequency stimulus (steep slope), which then relaxes back to its steady state (DC) value. These results support the hypothesis that type B neurons are more sensitive to dynamic changes than type A neurons. Table 1 shows that the average overshoot for a 600-ms ramp was about threefold greater in type B neurons compared with type A.

Spike discharge modulation

The low-frequency (0.4 Hz) hyperpolarized input resistances, R_h (0.4 Hz), of type A and B neurons are only slightly different (Table 1); however, at rest during the spontaneous firing of action potentials, the input resistance, R_{active} (0.4 Hz), of type B cells was 60% of type A. This suggests that the voltage dependent conductances of type B neurons are more open during spontaneous activity than in type A cells, which will lead to smaller potential excursions during spike discharge modulation by current input to the soma.

Although the spike discharge sensitivity to current input of type A and B neurons is about the same [see Table 1, $\delta IF / \delta I$ (0.4 Hz)], the sensitivity of type B neurons with respect to changes in the membrane potential is enhanced nearly twofold [see $\delta IF / \delta V$ (0.4 Hz), Table 1]. This is an important effect for synaptic inputs on small dendrites and should cause an overall increased sensitivity in type B neurons to afferent synaptic input. Furthermore, the higher sensitivity of type B neurons means that in these neurons, changes in firing rate are highly dependent on the membrane potential and thus tend to synchronize with an imposed sinusoidal stimulus.

Table 1 illustrates that type A neurons at rest show a 20% increase in their modulation amplitude (δIF) between 0.4 [δIF (0.4 Hz)] and 4 Hz [δIF (4 Hz)]. By contrast type B neurons show a 40% increase over the same frequency range. Our considerations have been limited to neurons that show good modulation at relative low input frequencies (<10 Hz); however, in the absence of modulation due to low firing rates or larger nonmodulating current inputs, the maximum spiking rates were also shown to increase with input frequency. Under these nonmodulating conditions, action potential responses behave more like signal detectors and do not provide information relative to a mean input that would be needed for a "push-pull" type of equilibrium control.

Since the action potential discharge rate is dependent on the membrane potential, the activation of ionic conductances by a membrane depolarization would be expected to alter the spike discharge modulation. Figure 9 (data, —) illustrates that both type A and B neurons are sensitive to a steady-state depolarizing current. At low frequencies, the constant current depolarization of the membrane potential decreases the amplitude of the spike discharge modulation of type A neurons, which then increases to approach the resting response at frequencies >10 Hz (Fig. 9A, —). In addition Fig. 9, E and F (—), shows that the phase functions of the modulated responses shift to higher frequencies with depolarization. This can be easily seen in Fig. 9E by comparing the phase at -20° , which changes from ~ 5 Hz at rest to >10 Hz during a depolarization.

Figure 9B shows the spike discharge modulation ampli-

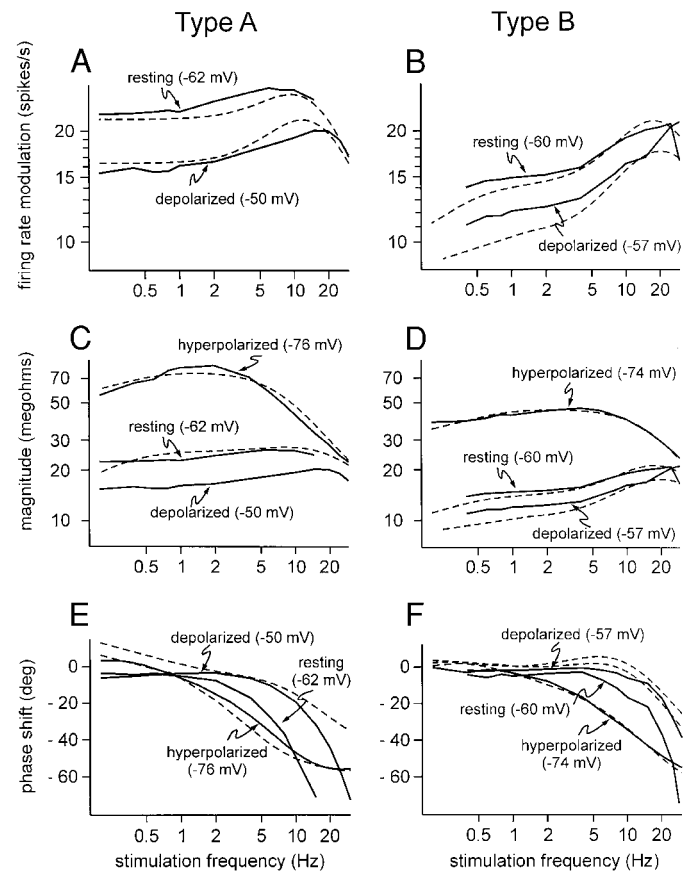


FIG. 9. Neuronal model description of spike discharge modulation. A and B: 2 superimposed magnitude functions (—) are shown for type A and B neurons (A and B) with model fits (---) that were based on the calibration from spikes/s to MΩ shown in C and D. The resting and depolarized spike discharge (spike/s) amplitude modulations show a greater increase in amplitude for the Type B (B) compared with the type A neuron. The model fits for the type A neuron in A were done with 1 potassium conductance, $g_K = 1.5$ nS, $v_n = -50$ mV, $s_n = 0.02$, and $t_n = 0.03$ s. The remaining parameters and type B fits are described in the following text. C and D: hyperpolarized impedance amplitudes for both type A and B neurons are shown along with calibrated spike discharge AM at resting and depolarized levels. ---, model fits with the following parameters: type A, $c_{soma} = 11$ pF, $A = 26.8$, $L = 0.55$, $g_{soma} = 0.3$ nS, $g_{K2} = 20$ nS, $v_q = -44$ mV, $s_q = 0.035$, $t_q = 3.4$ s, $r_q = 0$; $g_{K1} = 50$ nS, $v_n = -34$ mV, $s_n = 0.06$, $t_n = 0.34$ s, $r_n = 0$; type B, $c_{soma} = 15$ pF, $a_{ratio} = 14$, $L = 0.37$, $g_{K1} = 11$ nS, $v_n = -58$ mV, $s_n = 0.17$, $t_n = 0.03$ s, $g_{K2} = 14$ nS, $v_q = -41$ mV, $s_q = 0.02$, $t_q = 1.1$ s, $r_q = 0$. These parameters were used in B, E and F: corresponding phase functions for C and D. The most hyperpolarized response was measured directly from the membrane potential deflection responses free of action potentials. The resting and depolarized cases were measured with spike discharge modulation. Note that the low-frequency impedance decreases with depolarization, however, as the frequency increases, the magnitude of the impedance approaches a maximum resonance frequency that is dependent on the membrane potential. The phase functions corresponding to the resonating amplitudes show a phase lead at low frequencies that crosses 0 and becomes a phase lag at high frequencies. At the most hyperpolarized levels, the resonance and phase lead disappear. The decrease in the impedance magnitude observed with depolarization has been modeled with 1 or 2 potassium conductances. See text for further details.

tude of a representative type B neuron that has a greater amplitude increase with frequency than observed in the typical type A neuron of Fig. 9A, both at rest (see Table 1) and during a depolarization. The type B phase functions of Fig. 9F also show positive values that are shifted to higher frequencies than the corresponding phases of the type A neuron of Fig. 9E. For example, in Fig. 9F a phase of -20°

at rest occurred at ~ 10 Hz, which shifted to ~ 20 Hz during a depolarization.

Hyperpolarized neurons

The hypothesis that spike discharge modulation is a measure of the membrane potential variation is supported by the preceding findings showing that the spike discharge modulation is altered in the same manner as the impedance when neurons are depolarized, namely there is a decrease in amplitude due to the activation of ionic conductances and a tendency to show some type of resonance phenomena (Moore et al. 1999). Similarly, a hyperpolarization should increase the input resistance and provide a near passive control measurement. Table 1 indicates that the input resistance determined with a pulse of current at hyperpolarized values increased about twofold over the resting input resistance in type B neurons and somewhat less in type A cells. This difference is consistent with the hypothesis that the mean level of active conductances during resting spontaneous activity are more prominent in type B compared with A neurons.

To test our use of spike discharge modulation as a measure of the membrane potential, we hyperpolarized neurons to abolish action potential firing and measure directly the sinusoidal membrane potential responses without relying on spike discharge modulation. Under these conditions, a moderate peak in the magnitude of the hyperpolarized impedance was observed at ~ 5 Hz or below as illustrated in Fig. 9, *C* and *D*. Thus since a passive neuron would not show a peak or resonance response, these moderately hyperpolarized neurons had only part of their active conductances turned off and it was possible to observe nonpassive resonant behavior (Moore et al. 1999) in the absence of action potentials. This occurred because the hyperpolarization of 10–15 mV was used to just block spontaneous action potentials. A further manifestation of resonant behavior can be seen in the phase functions that are slightly positive at low frequencies and have a zero crossing near the peak of the resonance after which they become more negative as the frequency increases.

The gain and phase functions (data, —) shown in Fig. 9, *C* and *D*, from neurons that were hyperpolarized to abolish action potentials show a magnitude that begins to decrease at lower frequencies than measured by spike discharge modulation at the resting potentials. This result is a manifestation of increase in membrane impedance due to a decrease in active conductances caused by the hyperpolarization. Finally, these findings indicate that both the modulation of the spike discharge frequency and the membrane potential data show similar behavior, namely an increase in the magnitude of the response as the stimulating frequency is increased. Therefore it is reasonable to interpret the spike discharge modulation as an approximation of changes in the membrane potential.

Quantitative interpretation of spike discharge modulation

We have presented spike discharge modulation data (Fig. 9, —) for a range of stimulating frequencies and membrane potential levels. Furthermore the spike discharge modulation amplitude was assumed to have a constant relationship at all measured frequencies with membrane potential deflections, the value of which was based on an estimation made at 0.4 Hz.

This method of calibration was chosen to test the hypothesis that spike discharge modulation can be interpreted with linear analysis if the stimulating current evokes membrane potential changes that are < 10 mV. The sinusoidal data were fitted with a single sine function at each stimulation frequency to give estimated gain and phase functions, namely an experimentally determined neuronal impedance over the frequency range 0.4 to ~ 10 Hz. It is this latter estimated impedance function that can be interpreted with a theoretical model (APPENDIX).

Thus the experimentally estimated impedance was fitted with a linearized neuronal model (theory, Fig. 9, - - -) to obtain estimates of biophysical parameters (see APPENDIX). The fitting was done with the nonlinear fitting procedures using Mathematica as previously described (Moore et al. 1999). Furthermore the theoretical analysis suggests that the increase in gain or amplitude observed in the data are consistent with the linear resonant behavior of the usual potassium voltage dependent conductances (APPENDIX). This conclusion is important to determine the linear versus nonlinear contributions of MVNn to the overall gain functions of vestibular networks.

A major difficulty in this analysis was the inability to determine the peak resonant frequency due to the frequency limitation of the measurement. Nevertheless increasing amplitudes are indicative of resonant phenomena and consistent with models of vestibular neurons (Av-Ron and Vidal 1999). The data of Fig. 9 were fitted with a neuronal model having two potassium conductances (g_{K1} and g_{K2}) that were uniformly distributed throughout the surface area of the neuron (Figs. 9, *C–F*). As a further test of the use of spike discharge modulation for impedance analysis, three neurons were investigated in the presence of TTX to abolish action potentials and measure the membrane potential directly at depolarized membrane potentials. These data showed behavior similar to spike discharge modulation including a decrease in impedance with a depolarization and a shift of a resonant peak to higher frequencies.

The ability of the preceding analysis to quantitatively describe the resting and depolarized spike discharge data, hyperpolarized responses, and results in TTX, supports the hypothesis that modulation of the discharge rate can be interpreted with a linearized neuronal model. As pointed out in METHODS, this comparison with the model requires a calibration between the firing rate and the membrane potential. Our calibration procedure requires that the hyperpolarized sinusoidal membrane potential and spike discharge data should asymptotically agree at high frequencies, as illustrated in Fig. 9. Nevertheless this calibration is difficult to evaluate at all frequencies and should be taken as an assumption of the model. This fixed calibration factor leads to a resting membrane impedance at low frequencies that was about one-half of that determined at more hyperpolarized levels.

The parameters used in the hyperpolarized impedance model fits of Fig. 9, *C* and *D*, for both type A and B neurons adequately describe the calibrated resting spike discharge modulation data. The resting and depolarized data of the type A neuron were fitted separately with a single potassium conductance having a different set of parameters (Fig. 9A); however, the type B data were fitted with a model having two potassium conductances that had the same parameters at all three potentials. Thus in both type A and B neurons, two potassium conductances were required to quantitatively fit the data at all membrane potentials. Although the magnitude functions

shown in these fits are reasonable descriptions, it is clear that the phase functions for spike discharge modulation (Fig. 9, *E* and *F*) are not adequately described. This inadequacy of the phase estimates is most likely due the variable sampling that is inherent when using instantaneous firing rates (see DISCUSSION).

DISCUSSION

These results suggest that both type A and B neurons of the medial vestibular nucleus are able to modulate action potential firing rates in a way that is dependent on their level of depolarization. Many type B neurons were not able to modulate well because of low firing rates as well as a tendency to show complicated plateau like action potentials. If type B neurons are to be identified with the irregular phasic neurons seen *in vivo*, then their ability to modulate would be limited by this variability. Thus type A neurons could be identified with tonic neurons and, as such, would be better suited as modulators of a firing rate. On the other hand, type B neurons respond more reliably at high frequencies. Thus they act as excellent signal detectors, in part due to their complex repertoire of nonlinear voltage dependent channels (Serafin et al. 1990, 1991b). Sensitivity of modulation varies with neurons, and there is no clear relation between the spontaneous discharge and the highest modulation frequency, although it must limit it.

The most significant differences between the type A and B neurons (Table 1) were found for the active membrane input resistances at 0.4 Hz and the sensitivity of the spike discharge modulation relative to the membrane potential ($\delta IF/\delta V$) but not the current ($\delta IF/\delta I$). An additional difference was found for the effect of stimulation frequency on spike discharge modulation, $\delta IF(4 \text{ Hz})/\delta IF(0.4 \text{ Hz})$; however, this effect was not as significant as the low-frequency findings (Table 1). This lack of significance was partly due to an inability to compare the two cell types at higher frequencies.

The preceding analysis of instantaneous firing rate modulation lends support to the hypothesis that some vestibular neurons behave like moderately tuned filters, which resonate to varying degrees dependent on individual membrane properties. This tuned or resonant behavior is directly determined by the linearized voltage-dependent membrane properties, which are correspondingly responsible for the gain enhancement of action potential firing rates with the stimulus frequency. Interestingly, although action potentials themselves are clearly nonlinear responses, the modulation of their discharge rate appears to be a linear process. It should be emphasized that the linearized responses of the voltage-dependent conductances are clearly not passive. Thus the underlying basis of these active responses are due to fundamentally nonlinear voltage-dependent processes, which can be linearized if the afferent inputs are sufficiently small. This type of response in a network has been referred to as "nonlinear" gain function that increases with frequency (Minor et al. 1999).

A recent study of the VOR (Minor et al. 1999) showed that inputs from regularly discharging afferents to the reflex pathway had a constant gain across input frequencies; however, other inputs had a gain that increased with frequency and were therefore modeled as a nonlinear process. Thus it appears that the overall gain of the reflex pathway is the sum of two processes, one linear and decreasing with frequency like a simple linear passive filter and another that is based on active

voltage-dependent conductances, that increases with frequency before decreasing, i.e., a resonance response or active dynamic filter. The experiments in this paper show that the resonant responses of individual medial vestibular nucleus neurons (MVNn) could be responsible for a large part of these frequency-dependent gain variations. In the case of type B neurons, the increase in the gain of the spike FM from 0.4 to 4 Hz is ~40%. This behavior suggests that the type B MVNn are moderately tuned active filters that promote high-frequency responses. The marked increase in VOR gain with increasing stimulus velocity that occurs at 4 Hz, in contrast to a constant VOR gain at 0.5 Hz (Minor et al. 1999), can be compared with our ramp experiments where increasing current levels were applied. In these experiments, the type B neurons showed greater nonlinear increases in spike discharge at high frequencies, namely with steep ramps, than for slow ramps that would evoke low-frequency responses. Interestingly most type A neurons did not show this type of nonlinearity.

The spike discharge modulation results (Fig. 9) show that the activation of voltage-dependent conductances with depolarization decreases the low-frequency impedance and shifts resonant behavior to higher frequencies. Correspondingly, the spike discharge modulation also shows a shift of the positive phase functions to higher frequencies. By comparison, the membrane potential responses of hyperpolarized neurons also show increased amplitudes, but phase functions that have little or no positive component. The values of the hyperpolarized membrane resistances (Table 1) are lower than previously reported values of >100 M Ω for both type A and B neurons (Serafin et al. 1991a). Part of this difference may be due to a remaining active potassium conductance as is suggested by the slight resonance observed for the hyperpolarized neurons of Fig. 9, *C* and *D*. Our measurements were not done at a sufficient hyperpolarization to turn off all of the active conductances, which could have given a larger value for the membrane resistance, i.e., the passive impedance of the neuron. The type B active input resistance values at rest were lower than type A (R_{active} , Table 1), which is consistent with a greater number of active ionic channels in type B cells. It may as well be linked with the reported difference in dendritic structure, namely that type B neurons have a larger cell body and greater number of branching dendrites compared with type A neurons (Serafin et al. 1993).

The tests of linearity displayed in Fig. 6 show that the amplitude of spike modulation for increasing currents was linear for currents <0.3 nA. The finding that the increase in modulation amplitude for the type B neuron remains parallel for three current levels strongly supports the argument that this effect, namely, an enhanced amplitude with increasing frequencies, is a linear response as long as the current stimulating level remains <0.3 nA. Thus the active voltage-dependent conductances are exerting their effects on the steady-state linear membrane impedance and thereby, directly influencing spike discharge behavior. These results are consistent with previous findings on chick vestibular neurons (du Lac and Lisberger 1995a), which generally show a linear increase in spike modulation amplitudes as the stimulating frequency is increased. Although spike discharge behavior is dependent on nonlinear voltage-dependent conductances, this does not mean that the modulated spike discharge responses with small signal inputs require a nonlinear analysis. Since the linearization of

Hodgkin-Huxley type neuronal models generally show highly resonant behavior, it is not surprising that the data obtained in this paper can be described in this manner, namely a piece-wise linear analysis.

If linear analysis provides an adequate description of the modulation of instantaneous firing rate, then the underlying membrane potential would be expected to show a similar result. It is difficult to rigorously verify this point because the presence of action potentials prevents the accurate measurement of sinusoidal membrane potential responses to small current inputs. However, membrane potential responses in the presence of few action potentials have been estimated by Fourier analysis in cortical neurons during sinusoidal analysis (Carandini et al. 1996). These data show a small but clear increase in amplitude with frequency (see Figs. 7 and 8) (Carandini et al. 1996) that actually passes through a maximum resonant value between 2 and 5 Hz. This resonance requires the presence of voltage-dependent conductances and cannot be quantitatively described by a passive model; however, contrary to what happens in our case, it is not quantitatively identical to the nonmodulated peak instantaneous firing rates measured from the same records (Carandini et al. 1996). Thus the discrepancy observed in cortical neurons between the membrane potential response and instantaneous firing rate is quantitative and appears to be a consequence of the nonlinearities associated with a lack of uniform modulation.

A nonlinear relationship between spiking rate and injected membrane current has been observed in many neurons for current levels that clearly increase the total membrane conductance, which in turn leads to membrane potential responses that decrease nonlinearly with depolarization. Thus the relationship between spike firing rate and membrane potential cannot be linear over wide ranges of membrane potential, which would suggest that the calibration between spike discharge modulation and membrane potential could be potential dependent. Nevertheless linear approximations are probably valid for the limited changes in the membrane potential that were used in these experiments. Although spike train encoding is likely to be nonlinear for large stimulus inputs, it seems likely that some vestibular neurons operate in a stimulus range (Figs. 6–8) that allows modulated linear responses. Nevertheless it should be pointed out that the slice preparation has significantly less synaptic input than present in intact systems, where background activity may depolarize neurons to membrane potentials that could lead to more nonlinear behavior.

The model fits of Fig. 9 show that the amplitude but not the higher frequency phase response can be reasonably well described by the linear response. The low-frequency phase responses do indicate a phase lead that crosses zero and becomes negative (phase lag) as the frequency increases. After the zero crossing, there is serious deviation from the model behavior (Fig. 9, *E* and *F*). The most likely reason for the phase discrepancy is insufficient and variable sampling intervals inherent in the instantaneous firing rate measurement. The standard procedure of taking the second action potential as the point in time for instantaneous firing rates causes a delay bias that progressively increases with frequency. This effect is significant because the conversion of a digital rate process to an unequally sampled analog response (IF) assumes that the time of sampling is at the end of the interval, which clearly gives an extra phase lag. For similar reasons, if the first action potential

is taken as the time point, there is a phase advance that also increases in frequency. This latter behavior is apparently the basis of the phase advance shown by some simple oscillator models (du Lac and Lisberger 1995a), which we have duplicated by using the latter procedure. Interestingly, a phase advance remains if the midpoint of the interval is used. In all these cases, the estimated phase does not accurately represent the response of a linear system; however, the standard procedure of taking the second time point appears to better reflect the qualitative behavior of neuronal transfer functions up to moderate frequencies.

It is interesting to compare the dynamical properties of regular versus irregular discharging canal afferents (Goldberg 2000) with those of type A and B neurons. Rotational stimulation has been used to obtain transfer functions (Anastasio and Correia 1988; Anastasio et al. 1985) showing that regular afferents have less phase difference referenced to head velocity than irregular afferents (Fernandez and Goldberg 1971). It has been suggested that the VOR needs a phase lead that increases with frequency to compensate for the phase lag caused by the delay in the reflex (Minor et al. 1999; Tabak et al. 1997). Compensatory phase advances between 1 and 10 Hz have not been consistently observed (Dickman and Correia 1989a,b; Highstein et al. 1996; Rabbitt et al. 1995); however, galvanic stimulation in squirrel monkeys (Goldberg et al. 1982) and a recent study of regular afferents in chinchillas (Hullar and Minor 1999) have shown such phase leads. In this latter study, the time of the instantaneous firing rate was the midpoint between impulses, which might exaggerate the phase advance (see preceding discussion of simple oscillator models used in du Lac and Lisberger 1995a). Nevertheless, it would appear that the MVNn will increase the phase lead up to the resonant peak, and this effect is more pronounced in type B versus A neurons.

Despite the limitations in the phase functions, a relatively simple linear model quantitatively describes the effect of changes in the resting membrane potential on the spike discharge modulation, which generally is greater in type B compared with A neurons. It would appear that the potential dependence of the voltage-dependent conductances is such that they are more activated at resting levels in B neurons than in A neurons. Both types of neurons show an enhancement of resonant behavior during a maintained depolarization, which provides a method to enhance the high-frequency responses of the overall network behavior. This range of dynamic filtering properties could compensate in part for the apparent input divergence of regular and irregular afferents to different second-order vestibular neurons (Chen-Huang et al. 1997; Goldberg 1991, 2000; Goldberg et al. 1984, 1987) since the principal determinant of the high-frequency responses would thus be the MVNns that would be capable of responding to both types of afferents. Type B neurons could enhance the flat response of regular afferents at high frequencies while type A cells could receive additional input from the more sensitive irregular inputs allowing more accurate control signals at low frequencies than would be provided from just their regular inputs.

In addition to the increase in the linear response as the frequency is increased, larger stimuli clearly evoke additional nonlinear behavior that is different in type B versus A neurons. The responses to current ramps illustrated in Figs. 7 and 8

show that the instantaneous firing rate responses are increased over their linear responses by steep ramps in type B cells. Similar behavior has been observed in some cortical neurons (Stafstrom et al. 1984), which also show a wide range of behaviors for different neuronal populations. Although the overshooting response is clearly nonlinear behavior for type B neurons in the medial vestibular nucleus, it is analogous to the enhanced response seen with linear sinusoidal analysis. It is interesting that the type A neurons appear to have nearly linear behavior for ramp stimuli that evoke large displacements in the membrane potential. Nevertheless large sinusoidal currents were shown to evoke nonlinear responses in type A neurons (see Fig. 6). These results suggest that both type A and B neurons remain linear for instantaneous firing rate information over a limited range of input stimuli; however, type B cells show an enhanced response at high frequencies for both linear and nonlinear stimuli. If the VOR dynamics have both linear and nonlinear components (Minor et al. 1999), these results would suggest that there could be a greater participation of type B versus A cells in the latter.

The membrane properties (Darlington et al. 1995; Dutia and Johnston 1998; Gallagher et al. 1985; Johnston et al. 1994) that may give rise to the different network functions have yet to be quantitatively determined. Developmental studies suggest that tonic firing behavior occurs principally in mature animals and is dependent on the potassium delayed rectifier (Desmadryl et al. 1986, 1997; Gamkrelidze et al. 1998; Peusner and Giaume 1998; Peusner et al. 1997), which is consistent with our finding that the potassium conductances may be different between type A and B neurons. Other experiments on the motoneurons found in the vestibuloocular system show a variety of firing properties (Gueritaud 1988) and passive electrotonic structures that are not correlated with morphological features (Durand 1989). Finally, there is ample evidence from action potential behavior that vestibular neurons have a wide range of voltage-dependent conductances (de Waele et al. 1993; du Lac and Lisberger 1995b; Llinás 1988; Serafin et al. 1990) that are capable of generating in realistic neuronal models most of the observed excitability behavior. The quantitative approach developed in this paper provides one way to assess the more general system behavior (Anastasio 1998; Robinson 1981), which could be extended to include more components in the VOR or other vestibular-related reflex pathways.

In summary, the purpose of comparing model predictions with the experimental impedance function was to test the hypothesis that the linear behavior of a neuronal model with only potassium conductances can describe the frequency domain data obtained using spike discharge modulation. Neuronal models with more active ionic conductances could also be investigated and eventually used to generate action potential responses. Our initial analysis has been restricted to show that this approach can be used in the presence of spontaneous activity over a limited range of mean membrane potentials that typically occur in situ. Finally, it was found that the linear responses of vestibular neurons are capable of showing a gain increase with frequency, which is more pronounced in presumed phasic neurons (type B) compared with tonic cells (type A). Physiologically these linear responses are likely to be enhanced by the nonlinearities observed in both type A and B neurons.

APPENDIX

Neuronal model

Neuronal models with active conductances can be extremely complex due to the number of different ionic conductances needed and the nature of their distribution throughout a dendritic structure. The purpose of the limited modeling done in this paper is to determine if subthreshold membrane potential changes estimated from modulation of the firing frequency can be interpreted with a minimal neuronal model having only potassium conductances. This model can quantitatively describe the spike discharge modulation evoked by small signal sinusoidal current inputs to determine if such linear membrane models would be sufficient to explain the gain enhancement at increasing frequencies observed in vestibular neurons. Our analysis shows that the resonance due to the interaction of the passive membrane properties and a single potassium conductance can increase the amplitude of the spike discharge modulation as the frequency is increased if it is assumed that there is an essentially linear relationship between the membrane potential change and modulation of discharge rate at all stimulating frequencies.

Since linearized neuronal models have been presented previously (Saint-Mleux and Moore 2000a,b), only a brief description will be given here. The basic passive structure is illustrated in Fig. 1B showing a soma and one equivalent dendritic cylinder. One or two uniformly distributed potassium ionic conductances were used, and these were described by a simplified Hodgkin-Huxley set of equations (Murphey et al. 1995). A Rall analytical model of single neurons was used to describe cable properties (Rall 1960). Parameter values for active and passive parameters were estimated with the linear analytical form of the complete model (Moore et al. 1999) having one or two potassium conductances, given by the following

$$Y_{\text{soma}}(V, f) = j2\pi f c_{\text{soma}} + g_{\text{soma}} + \sum_p g_p \{x_\infty(V) + (V - V_p)(dx_\infty/dV)/(1 + j2\pi f \tau_x)\}$$

where Y_{soma} is the admittance of the somatic compartment, $j = \sqrt{-1}$, c_{soma} is the somatic capacitance, g_{soma} is the passive leakage conductance of the soma, g_p is a generic voltage-dependent ionic conductance with a reversal potential of V_p and whose kinetics is governed by the unitless variable, x , which has a steady-state value of x_∞ . Thus at the half-activation voltage, v_{x^*} , $x_\infty = 1/2$, s_x is the slope of x versus voltage, r_x is the normalized slope of the time constant, τ_x , versus voltage, and t_x is the time constant, τ_x . In this paper, g_p represents potassium conductances (g_{K1} or g_{K2}) where the variable, x , is n or q (Moore et al. 1999; Murphey et al. 1995) and f is the frequency in Hertz.

Finally,

$$Y_t = Y_{\text{soma}} + A^* g_{\text{soma}} (\sqrt{(Y_{\text{soma}}/g_{\text{soma}})/L}) \tanh(L(\sqrt{(Y_{\text{soma}}/g_{\text{soma}})}) \quad (A1)$$

where Y_t is the total admittance ($\delta I/\delta V = 1/Z_{\text{active}}$) of the neuron measured from the soma, A is the ratio of the total area of the dendritic compartments to the soma, and L is the electrotonic length (Moore et al. 1999).

L. Ris is Research Assistant of the Belgian National Fund for Scientific Research.

This research was supported by CNRS (France) and by grants from the Belgian National Fund for Scientific Research, the Belgian Fund for Scientific Medical Research, the Queen Elisabeth Fund for Medical Research, and the Interuniversity Poles of Attraction Programme—Belgian State, Prime Minister's Office—Federal Office for Scientific, Technical and Cultural Affairs.

REFERENCES

- ANASTASIO TJ. Analysis and neural network modeling of the nonlinear correlates of habituation in the vestibulo-ocular reflex. *J Comput Neurosci* 5: 171–190, 1998.

- ANASTASIO TJ AND CORREIA MJ. A frequency and time domain study of the horizontal and vertical vestibuloocular reflex in the pigeon. *J Neurophysiol* 59: 1143–1161, 1988.
- ANASTASIO TJ CORREIA MJ, AND PERACHIO AA. Spontaneous and driven responses of semicircular canal primary afferents in the unanesthetized pigeon. *J Neurophysiol* 54: 335–347, 1985.
- AV-RON E AND VIDAL PP. Intrinsic membrane properties and dynamics of medial vestibular neurons: a simulation. *Biol Cybern* 80: 383–392, 1999.
- BABALIAN A, VIBERT N, ASSIÉ G, SERAFIN M, MÜHLETHALER M, AND VIDAL PP. Central vestibular networks in the guinea-pig: functional characterization in the isolated whole brain in vitro. *Neuroscience* 81: 405–426, 1997.
- CARANDINI M, MECHLER F, LEONARD CS, AND MOVSHON JA. Spike train encoding by regular spiking cells of the visual cortex. *J Neurophysiol* 76: 3425–3441, 1996.
- CHEN-HUANG C, MCCREA RA, AND GOLDBERG JM. Contributions of regularly and irregularly discharging vestibular-nerve inputs to the discharge of central vestibular neurons in the alert squirrel monkey. *Exp Brain Res* 114: 405–422, 1997.
- CURTHOYS IS. The response of primary horizontal semicircular canal neurons in the rat and guinea-pig to angular acceleration. *Exp Brain Res* 47: 286–294, 1982.
- DARLINGTON CL, GALLAGHER JP, AND SMITH PF. In vitro electrophysiological studies of the vestibular nucleus complex. *Prog Neurobiol* 45: 335–346, 1995.
- DESMADRYL G, CHAMBARD JM, VALMIER J, AND SANS A. Multiple voltage-dependent calcium currents in acutely isolated mouse vestibular neurons. *Neuroscience* 78: 511–522, 1997.
- DESMADRYL G, RAYMOND J, AND SANS A. In vitro electrophysiological study of spontaneous activity in neonatal mouse vestibular ganglion neurons during development. *Brain Res* 390: 133–136, 1986.
- DE WAELE C, SERAFIN M, KHATEB A, YABE T, VIDAL PP, AND MÜHLETHALER M. Medial vestibular nucleus in the guinea-pig: apamin-induced rhythmic burst firing—an in vitro and in vivo study. *Exp Brain Res* 95: 213–222, 1993.
- DICKMAN JD AND CORREIA MJ. Responses of pigeon horizontal semicircular canal afferent fibers. I. Step, trapezoid, and low-frequency sinusoid mechanical and rotational stimulation. *J Neurophysiol* 62: 1090–1101, 1989a.
- DICKMAN JD AND CORREIA MJ. Responses of pigeon horizontal semicircular canal afferent fibers. II. High-frequency mechanical stimulation. *J Neurophysiol* 62: 1102–1112, 1989b.
- DU LAC S AND LISBERGER SG. Cellular processing of temporal information in medial vestibular nucleus neurons. *J Neurosci* 12: 8000–8010, 1995a.
- DU LAC S AND LISBERGER SG. Membrane and firing properties of avian medial vestibular nucleus neurons in vitro. *J Comp Physiol* 176: 641–651, 1995b.
- DURAND J. Intracellular study of oculomotor neurons in the rat. *Neuroscience* 30: 639–649, 1989.
- DUTIA MB AND JOHNSTON AR. Development of action potentials and apamin-sensitive after-potentials in mouse vestibular nucleus neurones. *Exp Brain Res* 118: 148–154, 1998.
- FERNANDEZ C AND GOLDBERG JM. Physiology of peripheral neurons innervating semicircular canals of the squirrel monkey. II. Response to sinusoidal stimulation and dynamics of peripheral vestibular system. *J Neurophysiol* 34: 661–675, 1971.
- GALLAGHER JP, LEWIS MR, AND SHINNICK-GALLAGHER P. An electrophysiological investigation of the rat medial vestibular nucleus in vitro. In: *Contemporary Sensory Neurobiology*, edited by Correia MJ and Perachio AA. New York: Liss, 1985.
- GAMKRELIDZE G, GIAUME C, AND PEUSNER KD. The differential expression of low-threshold sustained potassium current contributes to the distinct firing patterns in embryonic central vestibular neurons. *J Neurosci* 18: 1449–1464, 1998.
- GOLDBERG JM. The vestibular end organs: morphological and physiological diversity of afferents. *Curr Opin Neurobiol* 1: 229–235, 1991.
- GOLDBERG JM. Afferent diversity and the organization of central vestibular pathways. *Exp Brain Res* 130: 277–297, 2000.
- GOLDBERG JM, FERNANDEZ C, AND SMITH CE. Responses of vestibular-nerve afferents in the squirrel monkey to externally applied galvanic currents. *Brain Res* 252: 156–160, 1982.
- GOLDBERG JM, HIGHSTEIN SM, MOSCHOVAKIS AK, AND FERNANDEZ C. Inputs from regularly and irregularly discharging vestibular nerve afferents to secondary neurons in the vestibular nuclei of the squirrel monkey. I. An electrophysiological analysis. *J Neurophysiol* 58: 700–718, 1987.
- GOLDBERG JM, SMITH CE, AND FERNANDEZ C. Relation between discharge regularity and responses to externally applied galvanic currents in vestibular nerve afferents of the squirrel monkey. *J Neurophysiol* 51: 1236–1256, 1984.
- GUERTAUD JP. Electrical activity of rat ocular motoneurons recorded in vitro. *Neuroscience* 24: 837–852, 1988.
- HIGHSTEIN SM, RABBITT RD, AND BOYLE R. Determinants of semicircular canal afferent response dynamics in the toadfish *Opsanus tau*. *J Neurophysiol* 75: 575–596, 1996.
- HULLAR TE AND MINOR LB. High-frequency dynamics of regularly discharging canal afferents provide a linear signal for angular vestibuloocular reflexes. *J Neurophysiol* 82: 2000–2005, 1999.
- JOHNSTON AR, MACLEOD NK, AND DUTIA MB. Ionic conductances contributing to spike repolarization and after-potentials in rat medial vestibular nucleus neurones. *J Physiol (Lond)* 481: 61–77, 1994.
- LEWIS MR, GALLAGHER JP, AND SHINNICK-GALLAGHER P. An in vitro brain slice preparation to study the pharmacology of central vestibular neurons. *J Pharmacol Methods* 18: 267–273, 1987.
- LEWIS MR, PHELAN KD, SHINNICK-GALLAGHER P, AND GALLAGHER JP. Primary afferent excitatory synaptic transmission recorded intracellularly in vitro from rat medial vestibular neurons. *Synapse* 3: 149–153, 1989.
- LLINÁS R. The intrinsic electrophysiological properties of mammalian neurons: insights into central nervous system function. *Science* 242: 1654–1664, 1988.
- MARMARELIS PZ AND MARMARELIS VZ. *Analysis of Physiological Systems: The White-Noise Approach*. New York: Plenum, 1978.
- MINOR LB, LASKER DM, BACKOUS DD, AND HULLAR TE. Horizontal vestibuloocular reflex evoked by high-acceleration rotations in the squirrel monkey. I. Normal responses. *J Neurophysiol* 82: 1254–1270, 1999.
- MOORE LE, CHUB N, TABAK J, AND O'DONOVAN M. NMDA induced dendritic oscillations during a soma voltage clamp of chick spinal neurons. *J Neurosci* 19: 8271–8280, 1999.
- MURPHEY CR, MOORE LE, AND BUCHANAN JT. Quantitative analysis of electrotonic structure and membrane properties of NMDA activated lamprey spinal neurons. *Neural Computat* 7: 486–506, 1995.
- PEUSNER KD, GAMKRELIDZE G, AND GIAUME C. Potassium currents and excitability in second-order auditory and vestibular neurons. *J Neurosci Res* 53: 511–520, 1998.
- PEUSNER KD AND GIAUME C. Ontogeny of electrophysiological properties and dendritic pattern in second-order chick vestibular neurons. *J Comp Neurol* 384: 621–633, 1997.
- QUADRONI R AND KNÖPFEL T. Compartmental models of type A and type B guinea pig medial vestibular neurons. *J Neurophysiol* 72: 1911–1924, 1994.
- RABBITT RD, BOYLE R, AND HIGHSTEIN SM. Mechanical indentation of the vestibular labyrinth and its relationship to head rotation in the toadfish *Opsanus tau*. *J Neurophysiol* 73: 2237–2260, 1995.
- RALL W. Membrane potential transients and membrane time constants of motoneurons. *Exp Neurol* 2: 503–532, 1960. In: *The Theoretical Foundation of Dendritic Function. Selected Papers of Wilfrid Rall*, edited by Segev I, Rinzel J, and Shepherd GM. Cambridge, MA: MIT Press, 1995.
- RIS L, HACHEMAOUI M, VIBERT N, GODAUX E, VIDAL PP, AND MOORE LE. Frequency modulation capabilities of vestibular neurons in guinea pig slices. *Abstract of the 28th Annual Meeting of the American Neuroscience Association, Los Angeles, CA, 1998*.
- ROBINSON DA. The use of control systems analysis in the neurophysiology of eye movements. *Annu Rev Neurosci* 4: 463–503, 1981.
- SAINT MLEUX B AND MOORE LE. Firing properties and electrotonic structure of *Xenopus* larval spinal neurons. *J Neurophysiol* 83: 1366–1380, 2000a.
- SAINT MLEUX B AND MOORE LE. Active dendritic membrane properties of *Xenopus* larval spinal neurons analyzed with a whole cell soma voltage clamp. *J Neurophysiol* 83: 1381–1393, 2000b.
- SERAFIN M, KHATEB A, DE WAELE C, VIDAL PP, AND MÜHLETHALER M. Low-threshold calcium spikes in medial vestibular nuclei neurons in vitro: a role in the generation of the vestibular nystagmus quick phase in vivo? *Exp Brain Res* 82: 187–190, 1990.
- SERAFIN M, DE WAELE C, KHATEB A, VIDAL PP, AND MÜHLETHALER M. Medial vestibular nucleus in the guinea-pig. I. Intrinsic membrane properties in brainstem slices. *Exp Brain Res* 84: 417–425, 1991a.
- SERAFIN M, DE WAELE C, KHATEB A, VIDAL PP, AND MÜHLETHALER M. Medial vestibular nucleus in the guinea-pig. II. Ionic basis of the intrinsic membrane properties in brainstem slices. *Exp Brain Res* 84: 426–433, 1991b.
- SERAFIN M, KHATEB A, VIBERT N, VIDAL PP, AND MÜHLETHALER M. Medial vestibular nucleus in the guinea-pig: histaminergic receptors. I. An in vitro study. *Exp Brain Res* 93: 242–248, 1993.

- SERAFIN M, RIS L, BERNARD P, MUHLETHALER M, GODAUX E, AND VIDAL PP. Neuronal correlates of vestibulo-ocular reflex adaptation in the alert guinea-pig. *Eur J Neurosci* 5: 1827–1830, 1999.
- SHIMAZU H AND PRECHT W. Tonic and kinetic responses of cat's vestibular neurons to horizontal angular acceleration. *J Neurophysiol* 28: 991–1013, 1965.
- STAFSTROM CE, SCHWINDT PC, AND CRILL WE. Repetitive firing in layer V neurons from cat neocortex in vitro. *J Neurophysiol* 52: 264–277, 1984.
- TABAK S, COLLEWIJN H, BOUMANS LJ, AND VAN DER STEEN J. Gain and delay of human vestibulo-ocular reflexes to oscillation and steps of the head by a reactive torque helmet. I. Normal subjects. *Acta Otolaryngol (Stockh)* 117: 785–795, 1997.
- VIBERT N, DE WAELE C, SERAFIN M, BABALIAN A, MUHLETHALER M, AND VIDAL PP. The vestibular system as a model of sensorimotor transformations. A combined in vivo and in vitro approach to study the cellular mechanisms of gaze and posture stabilization in mammals. *Prog Neurobiol* 51: 243–286, 1997.
- WOLFRAM S. *The Mathematica Book* (4th ed.). New York: Cambridge Univ. Press, 1999.